



## CHAPTER IV

### NOVEL ELECTRODES FOR SUPERCAPACITORS FROM POLYBENZOXAZINE-DERIVED CARBON AEROGEL

#### 4.1 Abstract

Polybenzoxazine, a high-performance phenolic resin, was used as a precursor for carbon aerogel electrode of supercapacitors. A cost-effective ambient drying was used for benzoxazine aerogel preparation. After the pyrolysis of benzoxazine aerogel under a nitrogen atmosphere, carbon aerogel was obtained. The BET surface area of the carbon aerogel was approximately 360 m<sup>2</sup>/g. The activation of the carbon aerogels was also investigated in order to compare the physical and electrochemical properties. The BET surface area of the activated carbon aerogels increased more than twice in comparison with the unactivated one. The electrochemical behaviors were studied by cyclic voltammetry, galvanostatic charge-discharge, and electrochemical impedance spectroscopy. The results showed that the polybenzoxazine-derived-carbon aerogel exhibited good electrochemical performance. A specific capacitance of the carbon aerogel electrode was 30 F/g obtained at current density 5 mA/cm<sup>2</sup>. The specific capacitance increased to 78 F/g at the same current density after carbon dioxide activation. Moreover, the best electrochemical behaviors with the specific capacitance of 109 F/g were obtained from the electrode prepared from carbon aerogel which underwent heat treatment at 300 °C in air. The electrochemical impedance spectroscopy as well as cyclic voltammetry was also confirmed those electrochemical behaviors.

**Keywords:** Carbon aerogel/ Polybenzoxazine/ Supercapacitor

## 4.2 Introduction

Currently, energy demand is increasing in our life; therefore, energy storage devices—batteries, capacitors and fuel cells—have been received great attention because they are good alternative power sources for electronic devices, electrical vehicles, digital telecommunication systems, and memory back-up systems, etc. Some problems found in these devices are low energy density, short life time and durability, high cost and toxic waste which limited their use.

Electrochemical supercapacitors are energy storage devices, which have a high specific capacitance and long life cycle. These devices can be categorized into two types according to their operation mechanisms: electrical double-layer capacitors (EDLCs) and pseudocapacitors. The former is based on charge separation at the electrode/electrolyte interface, whereas the latter is based on Faradaic redox reaction in the electrode surface formed with electroactive materials [1]. The materials studied for capacitors have been mainly of three types: carbon, metal oxide, and conducting polymers. Carbon aerogels are promising materials as electrodes for EDLCs due to their high performance and low cost [2].

Carbon aerogels normally are obtained via polycondensation of resorcinol and formaldehyde using acid or base as a catalyst [3]. However, costly raw materials and tedious preparation time are the limitations for a commercial application. In this study, polybenzoxazine, a high-performance phenolic resin, is considered to be a precursor for carbon aerogel preparation because of its unique characteristics such as excellent dimensional stability and low water absorption [4]. Moreover, the facile synthesis approach adapted from the solventless method reported by Ishida *et al.* allows for scale-up production. Additionally, the surface characteristics of carbon aerogels—pore volume, pore size distribution, and specific surface area—can be varied by changing concentration and type of precursors of benzoxazine and/or catalyst.

The purposes of this work are to fabricate the carbon aerogel electrodes for supercapacitors by using polybenzoxazine, a high-performance phenolic resin, as a precursor. The physical and electrochemical properties of the electrodes will be investigated. In order to compare the electrochemical properties, the activated carbon aerogel will also be studied.

## 4.3 Experimental

### 4.3.1 Materials

All chemicals were used without further purification. Bisphenol-A was purchased from Aldrich, Germany. Triethylenetetramine (TETA) was purchased from FACAI Group Limited, Thailand. Formaldehyde solution (37% by weight) and sulphuric acid (95-97% H<sub>2</sub>SO<sub>4</sub> analytical grade) were purchased from Merck, Germany. *N,N*-Dimethylformamide (DMF) was purchased from Labscan Asia Co., Ltd., Thailand.

### 4.3.2 Measurements

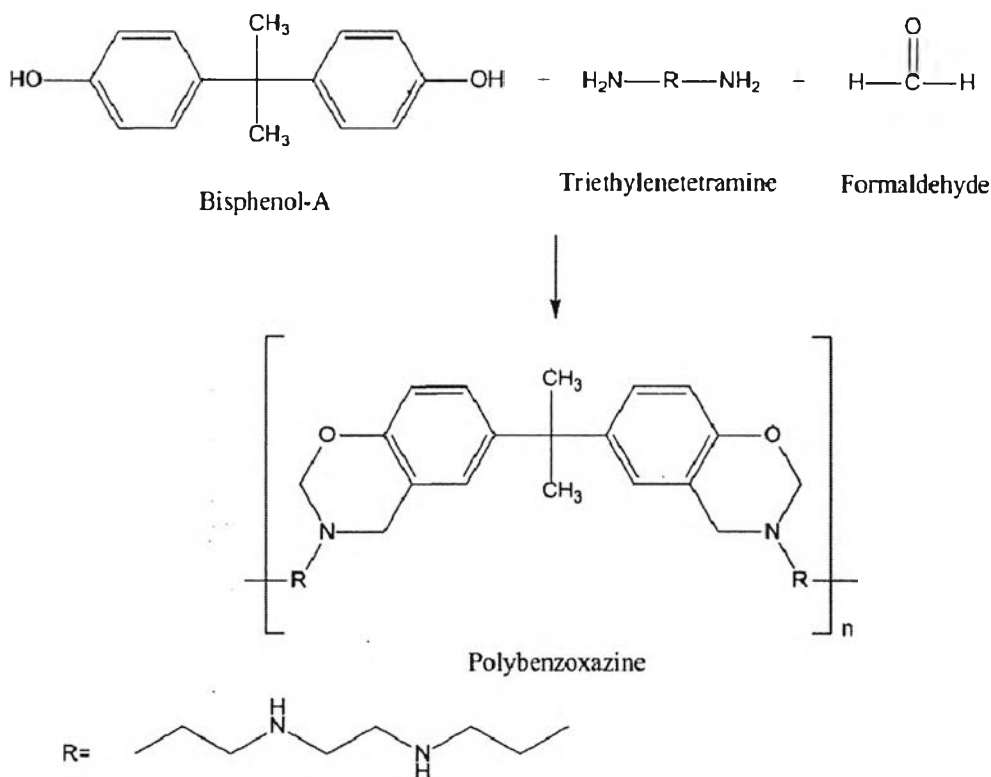
Thermal behaviors of polybenzoxazine aerogel were determined with differential scanning calorimetry (DSC), Perkin Elmer DSC7; The sample was heated from ambient temperature to 300 °C at a heating rate of 10 °C/min under nitrogen flow rate of 10 ml/min. Thermogravimetric analysis was also conducted with Perkin Elmer Thermogravimetric/Differential Thermal Analyzer (TG-DTA) where the sample was heated from ambient temperature to 900 °C at a heating rate of 20 °C/min under nitrogen flow rate of 50 ml/min. FT-IR spectra of polybenzoxazine precursor and carbon aerogel were recorded on a Nicolet Nexus 670 FT-IR spectrometer using KBr pallet technique. The field emission scanning electron microscope (FE-SEM, HITACHI S4800) was used to study the microstructure of carbon aerogel, the samples were coated with platinum under vacuum prior to investigation. BET surface area and pore size distribution of all carbon aerogels were calculated from nitrogen adsorption isotherms at 77 K using a Quantachrome/Autosorb-1 Surface Area Analyzer based on the Brunauer–Emmett–Teller (BET) and Barret-Joyner-Halenda (BJH) methods, respectively. For all electrochemical measurements, the electrochemical test cell consisted of graphite sheets as current collectors and two carbon aerogel electrodes separated by microporous polyethylene membrane. The carbon aerogel electrodes were soaked in 3M H<sub>2</sub>SO<sub>4</sub> electrolyte for 24 hr before measurement to ensure complete filling of the porous electrodes [5, 13]. The electrochemical properties were measured by a computer-controlled potentiostat/galvanostat (Autolab PG-STAT 30 with GPES software). Cyclic voltammograms were performed in the potential range of -1.0 V to 1.0 V with various scan rates. For galva-

nostatic charge/discharge measurement, the testing cell was charged with current density of  $5 \text{ mA/cm}^2$  up to 1 V and discharged with  $5 \text{ mA/cm}^2$  down to 0 V [5]. Electrochemical impedance spectroscopy measurements were carried out by Autolab PG-STAT 30 with FRA software in the frequency range of 10 kHz to 10 mHz with a sinusoidal signal of 10 mV. All of the electrochemical measurements were performed at room temperature.

#### 4.3.3 Methodology

##### 4.3.3.1 Synthesis of Polybenzoxazine Aerogels

The synthesis of polybenzoxazine precursor was started by dissolving Bisphenol-A (2.3075 g) in *N,N*-dimethylformamide (DMF) (15.00 g) and stirring continuously. Formaldehyde solution (3.2824 g) was then added into the bisphenol A solution. The solution was kept under low temperature by using ice bath. TETA (1.7388 g) was subsequently added dropwise into the mixture followed by continuous stirring for 1 hr until homogeneous yellow viscous liquid was obtained. The molar ratio of bisphenol-A:formaldehyde:TETA was 1:4:1. The synthetic reaction is shown in Scheme 4.1. Next, the precursor was filled in a vial with seal and placed in an oven at  $80^\circ\text{C}$  for 72 hr in a close system to generate benzoxazine aerogels. The benzoxazine aerogels were cut into disc shape and then dried at ambient temperature followed by placing in an oven at  $160^\circ$  and  $180^\circ\text{C}$  for 3 hr at each temperature and  $200^\circ\text{C}$  for 2 hr in order to polymerize benzoxazine aerogel.



**Scheme 4.1** Preparation of polybenzoxazine precursor.

#### 4.3.3.2 Preparation of Carbon Aerogel Electrodes

The benzoxazine aerogels were cut into a disc shape electrode and then pyrolyzed under a nitrogen flow rate of 600 cm<sup>3</sup>/min. The heating profile was as follows: heating from room temperature to 250°C in 60 min, 250° to 600°C in 300 min, 600° to 800°C in 60 min, and holding at 800°C for 60 min and finally cooling down to room temperature. The carbon aerogel electrodes were heat treated at 300°C in air for 120 min to modify the electrode surface and to improve affinity with the electrolyte [5].

Activated carbon aerogel (ACA) was prepared by carbonization of carbon aerogel with carbon dioxide at 900°C for 180 min.

#### 4.3.3.3 *Characterization of Polybenzoxazine Precursor and Carbon Aerogel Electrodes*

The chemical structure of benzoxazine precursor was characterized by Fourier transform infrared (FT-IR) spectroscopy. The thermal behaviors were measured using DSC and TG-DTA.

The surface area of carbon aerogels and activated carbon aerogels were calculated from nitrogen adsorption isotherms at 77 K based on the Brunauer–Emmett–Teller (BET) method and the pore size distribution was calculated with the adsorption data based on the Barret-Joyner-Halenda method (BJH). The surface morphology was characterized using scanning electron microscope (SEM).

For electrochemical measurement, the galvanostatic charge/discharge, cyclic voltammetry (CV) and electrochemical impedance spectroscopy (EIS) were determined. All of the electrochemical measurements were performed at room temperature.

### 4.4 Results and discussions

#### 4.4.1 Thermal Behaviors of Polybenzoxazine Precursors

The curing behaviors of polybenzoxazine were examined by DSC. The DSC thermogram shows the broad exotherm at 238 °C as shown in Figure 4.1 due to the ring opening polymerization of cyclic benzoxazine precursor. After the precursor was fully polymerized, the exotherm completely disappeared indicating that the ring opening of oxazine ring was completed. This result was similar to that reported by Takeichi and coworker [6].

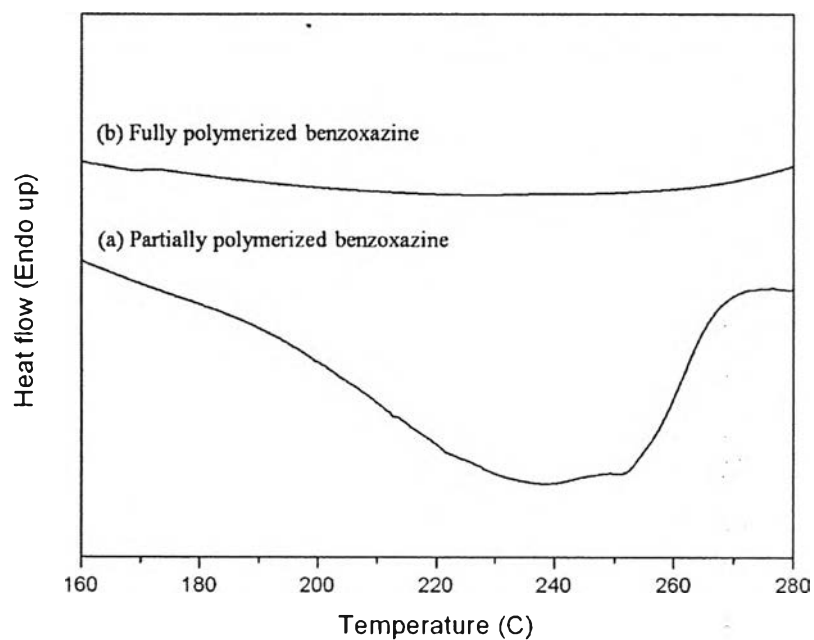


**Figure 4.1** DSC thermograms of polybenzoxazine precursor.

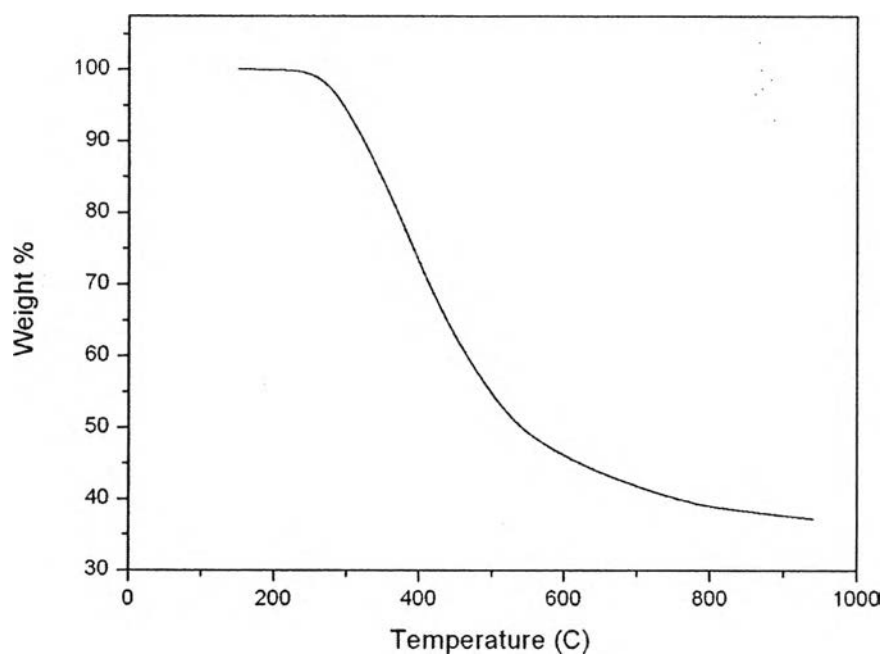


**Figure 4.2** TGA thermogram of polybenzoxazine precursor.

In Figure 4.2, the TGA thermogram shows the thermal stability of polybenzoxazine. The decomposition temperature began at 260 °C with the maximum mass loss rate in the temperature range of 260-600 °C. The result was in accordance with our previous study [7].

#### 4.4.2 The Chemical Structure of Polybenzoxazine Precursors

The chemical structure of benzoxazine precursor was examined by FTIR spectra as shown in Figure 4.3. The characteristic absorption bands at 1234-1238  $\text{cm}^{-1}$  (asymmetric stretching of C-O-C of oxazine), 1187  $\text{cm}^{-1}$  (asymmetric stretch of C-N-C) and 1334-1340  $\text{cm}^{-1}$  ( $\text{CH}_2$  wagging) were observed (Figure 4.3(a)). Additionally, the characteristic absorption assigned to the stretching of trisubstituted benzene ring at 1511  $\text{cm}^{-1}$  and the out-of-plane bending vibrations of C-H at 943-949  $\text{cm}^{-1}$  were detected, indicating the presence of the cyclic benzoxazine structure in the backbone of the precursor [8]. After polymerization at 200 °C, the intensity of those characteristic absorption bands decreased due to the ring opening polymerization was completed as shown in Figure 4.3(b) [6].

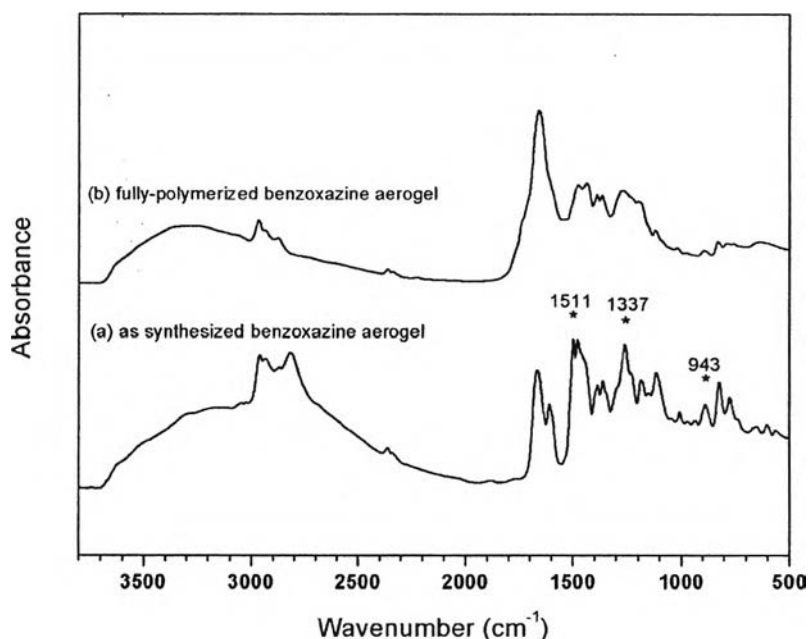


**Figure 4.3** FTIR spectra of polybenzoxazine precursors.



#### 4.4.3 Surface Characterization of Polybenzoxazine-Derived Carbon Aerogel

The surface area, pore volume and pore diameter of carbon aerogels are summarized in Table 4.1. It can be seen that the activated carbon aerogel had a high surface area with large amount of micropores whereas the non-activated sample had lower surface area, but larger pore size. The carbon aerogel had small amount of micropores. After the activation of carbon aerogel under carbon dioxide at 900 °C, the micropores had been introduced into the carbon aerogel, resulting in high surface area [9-12]. For the carbon aerogel with heat treatment in air at 300 °C, the surface area and porosity were similar [5]. Moreover, the pore diameter of all carbon aerogels prepared from polybenzoxazine precursor was in the range of 2-6 nm which was suitable for use as an electrode material in supercapacitors [5, 13].

**Table 4.1** Surface area, pore volume and pore diameter of carbon aerogels prepared from benzoxazine precursor

Parameter	CA	Heat-treated CA	Activated CA
BET surface area (m <sup>2</sup> /g)	360	372	910
Total pore volume (cm <sup>3</sup> /g)	0.24	0.25	0.54
Average pore size (nm)	2.69	2.65	2.40
Micropore volume (cm <sup>3</sup> /g)	0.14	0.16	0.40
Mesopore volume (cm <sup>3</sup> /g)	0.13	0.11	0.17
*Mesoporosity (%)	54.2	44.0	31.5
*Microporosity (%)	58.3	64.0	74.1

\*Mesoporosity = (mesopore volume/total pore volume) × 100

\*Microporosity = (micropore volume/total pore volume) × 100

#### 4.4.4 Morphology of Carbon Aerogels and Activated Carbon Aerogels

The SEM micrographs reveal the porous structure of the carbon aerogels prepared from polybenzoxazine via ambient drying as shown in Figure 4.4 (a)-(c). The structure of the carbon aerogel without heat treated at 300 °C in air composed of interconnected particles in three-dimension network containing continuous macropore, as shown in Figure 4.4(a) and (b), respectively. In case of the activation of carbon aerogels prepared by heat treated carbon aerogel with CO<sub>2</sub> at 900 °C, the micrograph also shows similar morphology compared with the unactivated one.

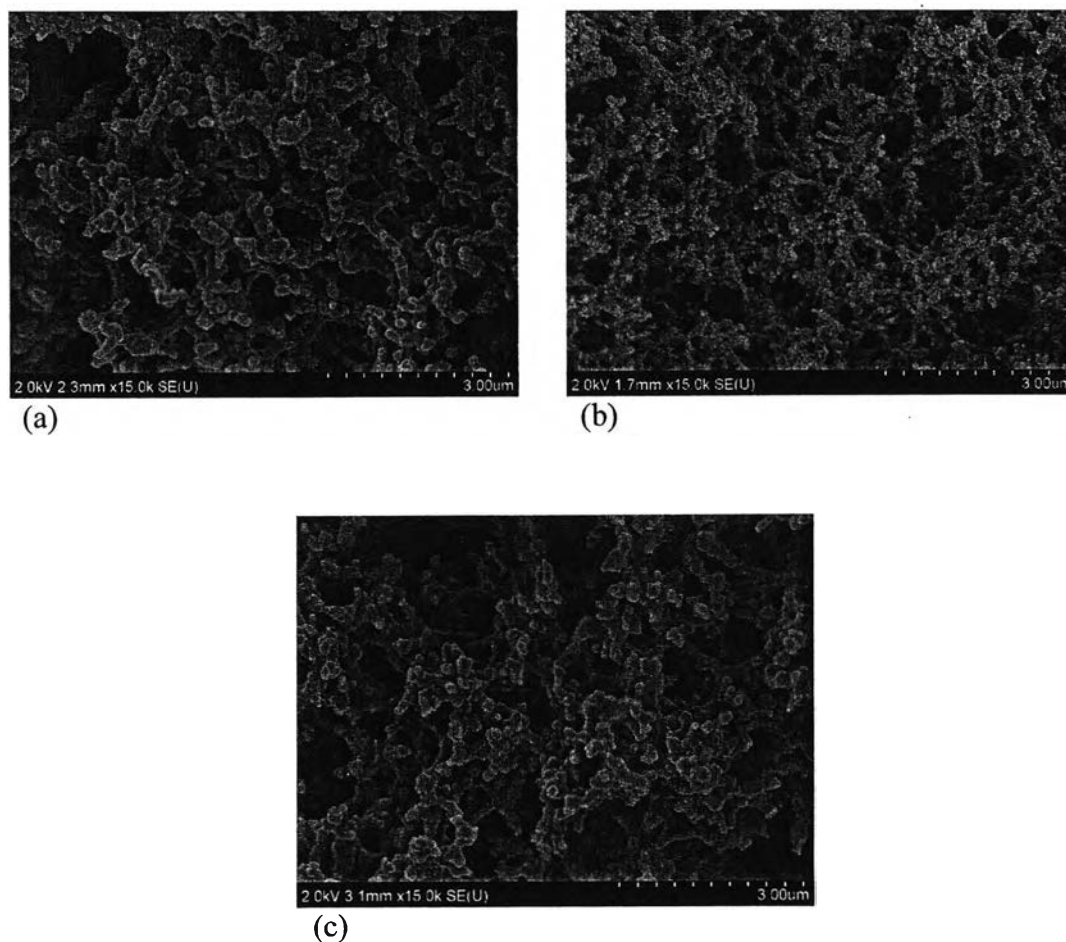
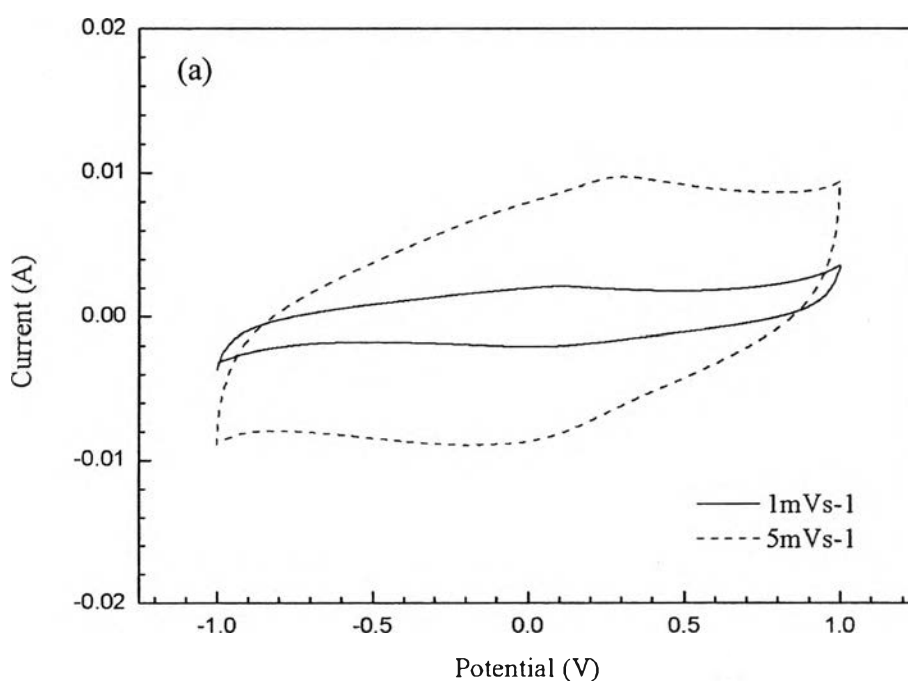


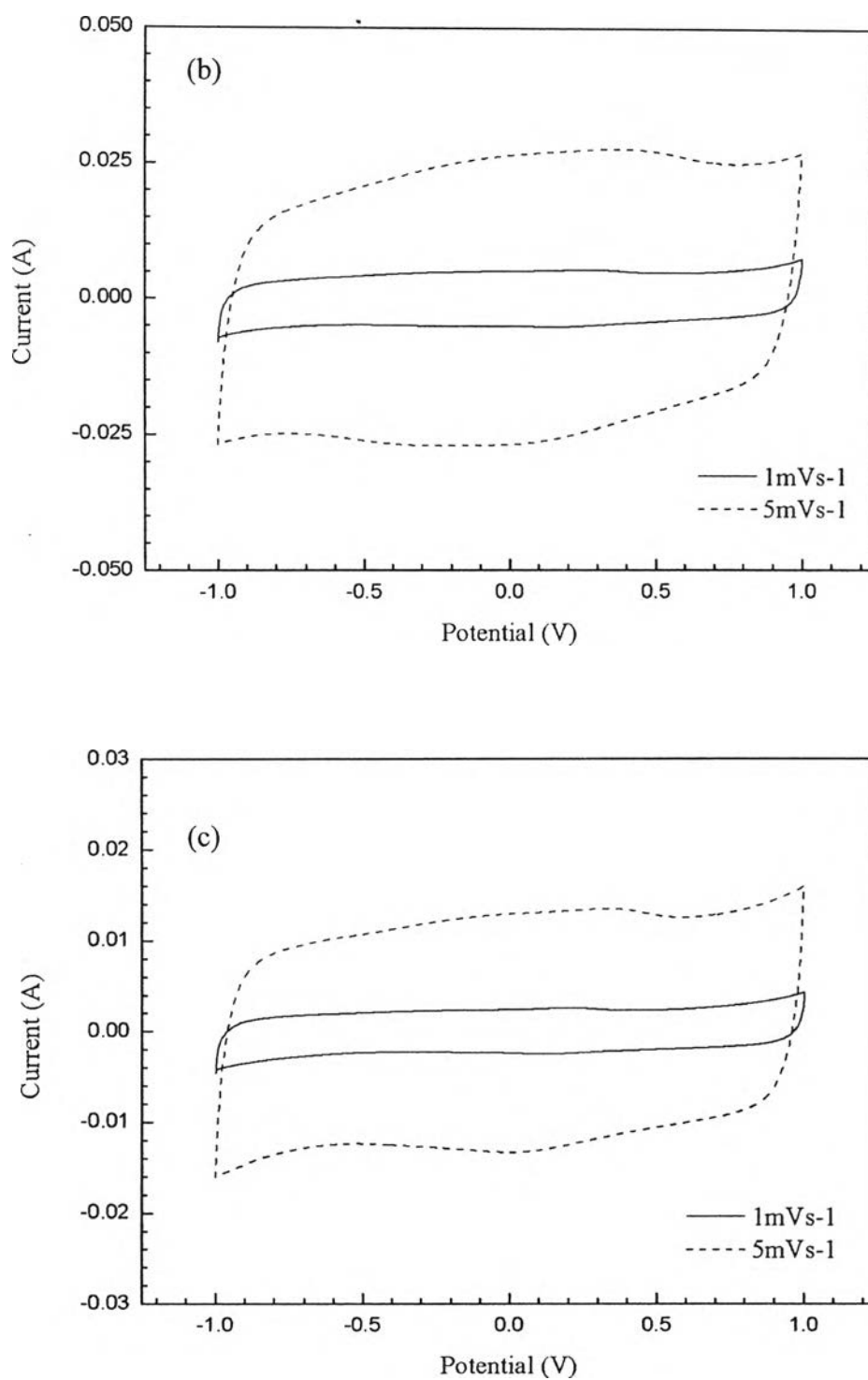
**Figure 4.4** SEM micrographs of synthesized carbon aerogels: (a) no heat-treated, (b) heat treated at 300 °C in air, and (c) activated at 900 °C under CO<sub>2</sub>.

#### 4.4.5 Electrochemical Characterizations

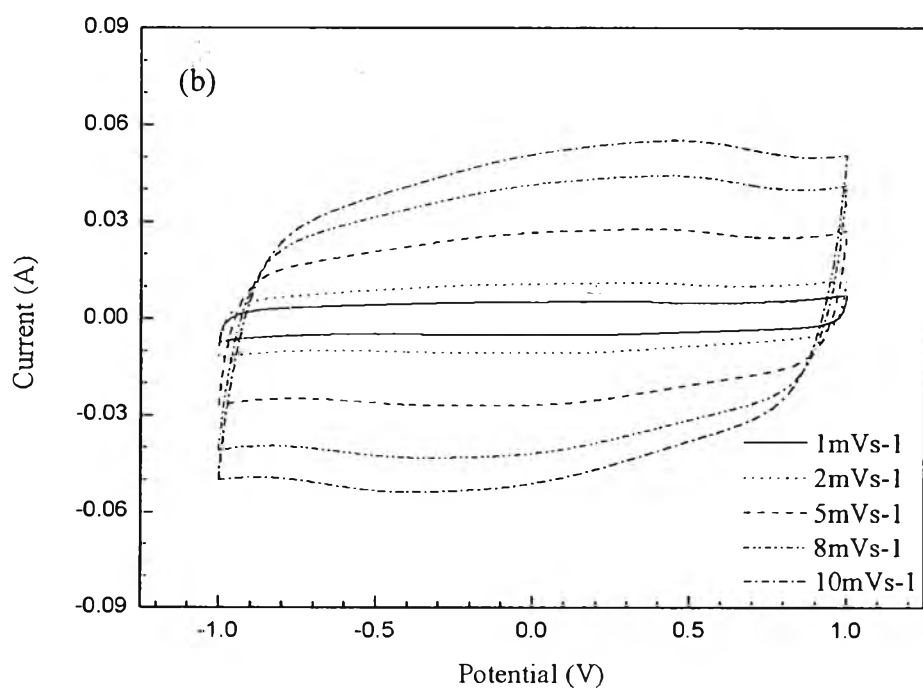
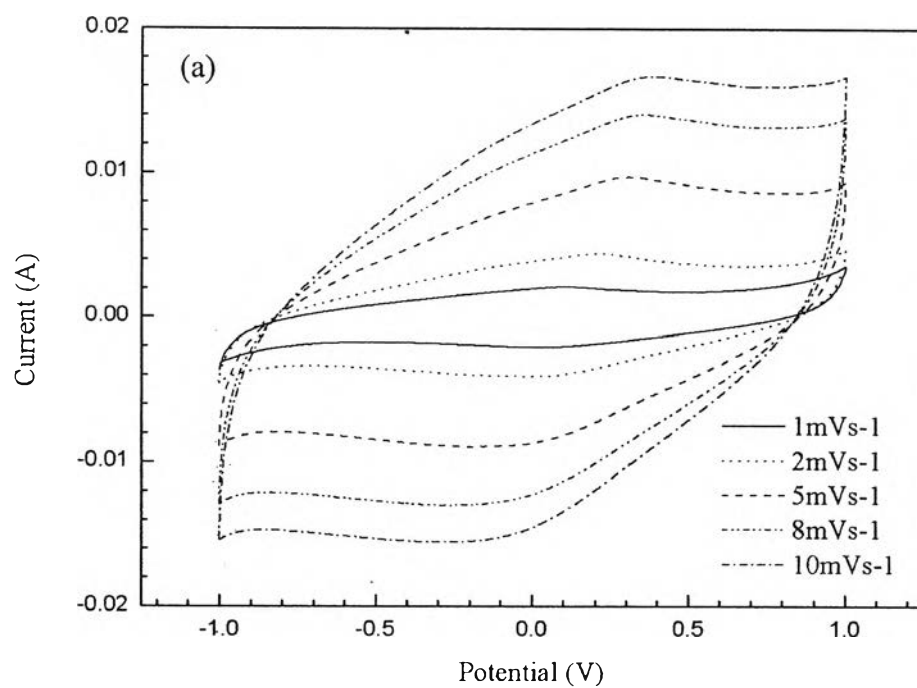
##### 4.4.5.1 Cyclic Voltammetry Behaviors

Figure 4.5 shows the cyclic voltammograms of the carbon aerogel electrodes obtained at a scan rate of 1 and 5 mV/s in 3M sulfuric acid. The figures show that the carbon aerogel electrodes particularly with heat-treatment at 300 °C in air and activated at 900 °C under carbon dioxide exhibited excellent electrochemical performances confirmed by a rectangular-like shapes of cyclic voltammograms, as shown in Figure 4.5 (b) and (c), suggesting that ions occupied some pores within the electrode for the electrochemical double layer formation [14]. In addition, they also imply that the charge/discharge processes of the electric double layer were highly reversible [14, 15]. For no heat-treated carbon aerogels, however, a small redox peak could be seen in the potential range of 0.1-0.4 V (Figure 4.5 (a)), which resulted from surface functional group. The pyrolysis temperature of 800 °C might not be enough to remove impurities completely from carbon network structure [5, 16]. As the scan rate increased, the rectangular shape became gradually depressed, because it was more difficult for the ions to transport into pores at high scan rate [17, 18].





**Figure 4.5** Cyclic voltammograms of carbon aerogel electrodes at a scan rate of 1 and 5 mV/s: (a) no heat treated, (b) heat-treated at 300 °C in air, and (c) activated at 900 °C under CO<sub>2</sub>.



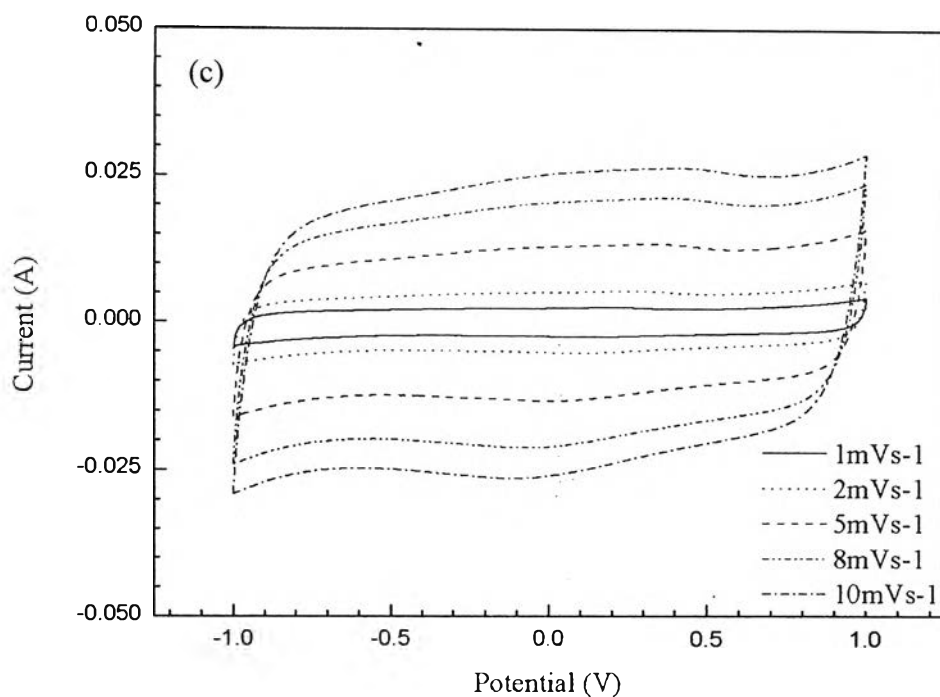


**Figure 4.6** Cyclic voltammograms of carbon aerogel electrodes at a scan rate of 1, 2, 5, 8, and 10 mV/s: (a) no heat treated, (b) heat-treated at 300 °C in air, and (c) activated at 900 °C under CO<sub>2</sub>.

#### 4.4.5.2 Charge-Discharge Behaviors

The specific capacitance ( $C$ ) of the carbon aerogel electrodes was calculated from the charge/discharge curve using the following equation [5, 7]:

$$C = \frac{i\Delta t}{m\Delta V} \quad (1)$$

where  $C$  is the specific capacitance (F/g),  $I$  is the constant current (A),  $t$  is time period (s),  $\Delta V$  is the potential difference (V), and  $m$  is the mass of carbon aerogel electrode (g).

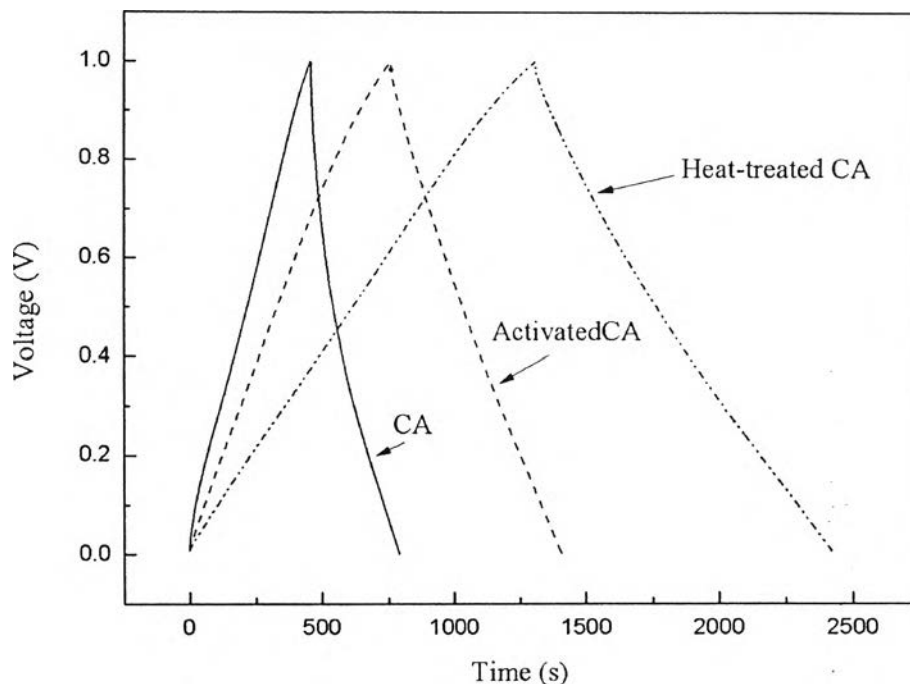


**Figure 4.7** Charge/discharge curves of the carbon aerogel electrodes measured at  $5 \text{ mA/cm}^2$ .

**Table 4.2** the specific capacitance of carbon aerogel electrodes calculated from discharge curves

Electrode	Specific capacitance (F/g)
Carbon aerogel	30
Heat-treated carbon aerogel	109
Activated carbon aerogel	78

It can be seen from Table 4.2 and Figure 4.7 that the activated carbon aerogel had large amount of micropores along with high surface area, resulting in higher specific capacitance than that of non-activated sample. The reason is that the polybenzoxazine derived carbon aerogel activated at  $900 \text{ }^\circ\text{C}$  under carbon dioxide had the average pore diameter approximately of  $2.40 \text{ nm}$ , which large enough for aqueous electrolyte to transport into pores to form the electrical double

layer [11-13]. However, the heat-treated carbon aerogel at 300 °C in air yield the highest specific capacitance due to its low micropore fraction, suitable pore size for electrical double layer formation and its pseudocapacitive behavior originated from surface functional group on carbon aerogel surface, which built up during the heat treatment at 300°C in air. Generally, the higher the specific surface area of the activated carbon, the higher the ability for charge accumulation; resulting in the higher the specific capacitance of the carbon electrodes [14, 16]. However, it is rather difficult to make a conclusive summary on the parameters that effect the charge accumulation since the nature and the porosity of the precursor also play important roles [14, 19].

#### 4.4.5.3 *Electrochemical Impedance Characteristics*

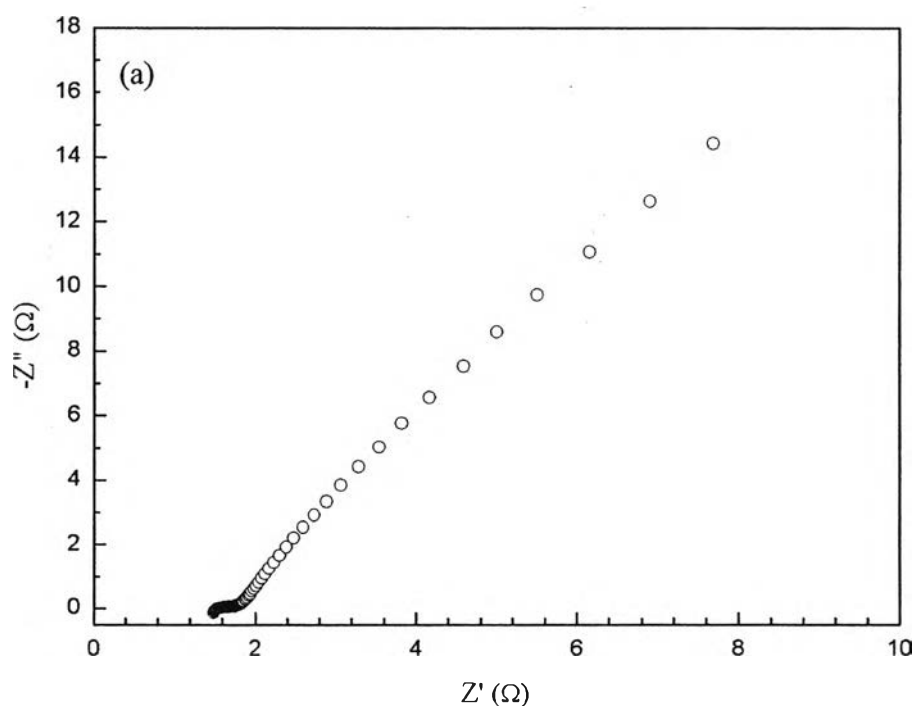
An electrochemical impedance measurement was carried out in the frequency range of 10 kHz to 10 mHz and the voltage between two electrodes was kept at 0 V during the measurement. Nyquist plots for these electrodes are presented in Figure 4.9. At high frequency, the intercept of the semicircle on the left of the real axis ( $Z'$ ) indicates the solution resistance,  $R_s$  and the intercept on the right of the real axis indicates the sum of the polarization resistance or charge transfer resistance,  $R_{ct}$ , and the solution resistance,  $R_s$ . The diameter of the semicircle is therefore equal to the charge transfer resistance,  $R_{ct}$  [20] which corresponds to the charge transfer process at the electrode-electrolyte interface [21].

It was found from Figure 4.8 (a)-(c) that the values read from the intercept on the left of the real axis of the electrochemical impedance spectrum were similar, indicating that all carbon electrodes had similar solution resistance. Although the heat-treated carbon aerogel had the highest capacitance, the diameter of the semicircles was less for the activated carbon aerogel than for the heat-treated carbon aerogel, indicating that the activated carbon had lower charge transfer resistance than heat-treated carbon aerogel. This could be explained for the heat-treated carbon aerogel that the imparted polarity might impede the ion mobility. However, the resistance did not play an essential role in affecting the specific capacitance during the constant current charge-discharge cycling, owing to the resistance has been excluded in capacitance calculation [22]. Hsieh and Teng reported that the specific capacitance of carbon fabric increased significantly with the extent of oxidation, however, the



inner resistance also found to be increased with the extent of oxidation due to the local changes of charge density and the increase in redox activity [22].

The straight line with a slope of  $45^\circ$  at a low frequency (Figure 4.8(a)), caused by diffusion of electrolyte ions within pores of the electrode [20, 23]. At low frequency, the imaginary part of the impedance of all carbon aerogel electrodes increased, showing the capacitive behavior of the supercapacitor [14, 19]. The slope also related to dispersed resistance,  $R$  and capacitance,  $C$ , originated from various pore structures in carbon aerogels. This interpretation was called a “transmission line model”, reported by De Livie (Figure 4.9) [9, 23, 25]. At a low frequency, the activated carbon aerogels exhibited a vertical line ( $90^\circ$ ) to the real axis, indicating an ideal capacitor behavior (Figure 4.8(c)). In contrast to the unactivated one, which had a high slope, indicating that the activated carbon aerogels had smaller diffusion resistance of electrolyte ions in the pore than the unactivated one, resulting in high specific capacitance as agree with the cyclic voltammograms and the charge/discharge curves [14, 20, 24].



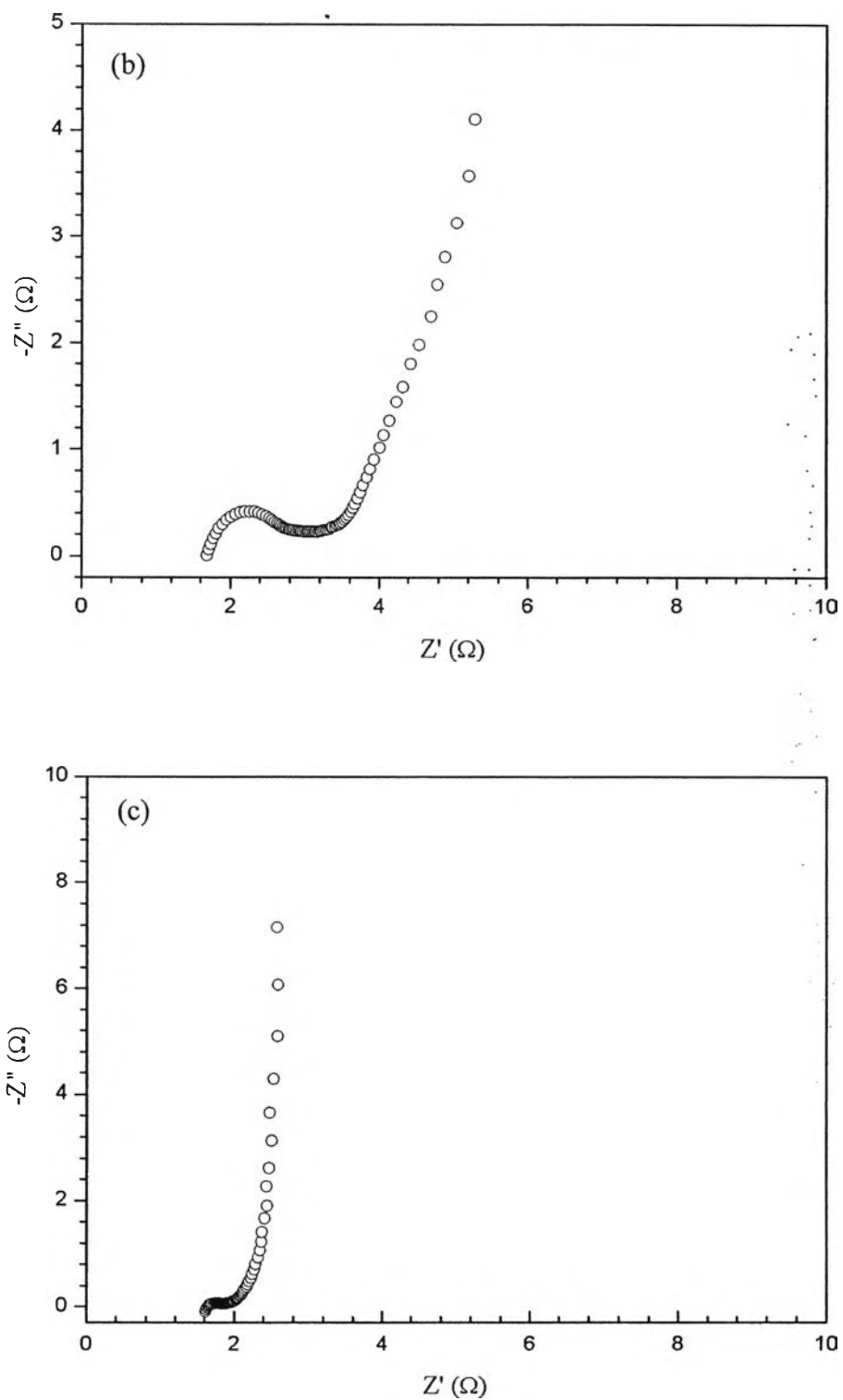


**Figure 4.8** Nyquist plots for carbon aerogel electrodes: (a) no heat-treated, (b) heat-treated at 300 °C in air, and (c) activated at 900 °C under  $\text{CO}_2$ .

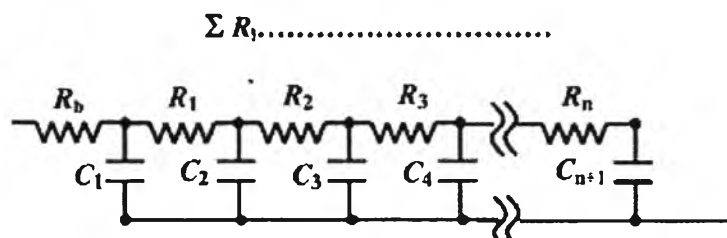


**Figure 4.9** The equivalent circuit of carbon aerogel electrodes [25].

### Conclusions

Carbon aerogel was successfully synthesized via ambient drying by using polybenzoxazine as a precursor. All carbon aerogel electrodes showed good electrochemical performances. The specific capacitance of the electrode fabricated from activated carbon aerogel was higher than that derived from the non-activated one due to its high useable surface area for electrical double layer formation. However, the heat-treated carbon aerogel electrode showed the best specific capacitance due to its pseudocapacitive behaviors.

### Acknowledgements

This thesis work is funded by the Petroleum and Petrochemical College, and the Center of Excellence for Petroleum, Petrochemicals, and Advanced Materials, Thailand. We would like to thank Associate Professor Suwabun Chirachanchai for electrochemical measurements.

### References

- [1] Conway, B.E. (1991) Transition from capacitors to battery behavior in electrochemical energy storage. *Journal of The Electrochemical Society*, 138(6), 1539-1548.
- [2] Pekala, R.W., Alviso, C.T., Kong, F.M., and Hulsey, S.S. (1992) Aerogels derived from multifunctional organic monomers. *Journal of Non-Crystalline Solids*, 145, 90-98.
- [3] Fairén-Jiménez, D., Carrasco-Marín, F., and Moreno-Castilla, C. (2006) Porosity and surface area of monolithic carbon aerogels prepared using alkaline

- carbonates and organic acids as polymerization catalyst. Carbon, 44, 2301-2307.
- [4] Ishida, H. and Allen, D. (1996) Physical and mechanical characterization of near-zero shrinkage polybenzoxazines. Journal of Polymer Science: Part B: Polymer Physics, 34, 1019–1030.
- [5] Kim, S.J., Hwang S.W., and Hyun S.H. (2005) Preparation of carbon aerogel electrodes for supercapacitor and their electrochemical characteristics. Journal of Material Science, 40, 725-731.
- [6] Takeichi, T., Kano, T., and Agag, T. (2005) Synthesis and thermal cure of high molecular weight polybenzoxazine precursors and the properties of the thermosets. Polymer, 46, 12172–12180.
- [7] Katanyoota, P., Chaisuwan, T., Wongchaisuwat, A., and Wongkasemjit, S. (2010) Novel polybenzoxazine-based carbon aerogel electrode for supercapacitors. Materials Science and Engineering B, 167, 36-42.
- [8] Dunkers, J. and Ishida, H. (1995) Vibrational assignments of N,N-bis(3,5-dimethyl-2-hydroxybenzyl)methylamine in the fingerprint region. Spectrochimica Acta Part A: Molecular and Biomolecular Spectroscopy, 51, 1061-1074.
- [9] Fang, B. and Binder, L. (2006) A modified activated carbon aerogel for high-energy storage in electrical double layer capacitors. Journal of Power Sources, 163, 616-622.
- [10] Baumann, T.F., Worsley, M.A., Yong-Jin Han, T., and Satcher, Jr. J. H. (2008) High surface area carbon aerogel monoliths with hierarchical porosity. Journal of Non-Crystalline Solids, 354, 3513-3515.
- [11] Frackowiak, E., and Béguin, F. (2001) Carbon materials for the electrochemical storage of energy in capacitors. Carbon, 39, 937-950.
- [12] Wang, J., Yang, X., Wu, D., Fu, R., Dresselhaus M.S., and Dresselhaus G. (2008) The porous structures of activated carbon aerogels and their effects on electrochemical performance. Journal of Power Sources, 185, 589-594.
- [13] Hwang, S.W. and Hyun, S.H. (2004) Capacitance control of carbon aerogel electrode. Journal of Non-Crystalline Solids, 347, 238-245.
- [14] Li, J., Wang, X., Wang, Y., Huang, Q., Dai, D., Gamboa, S., and Sebastian, P.J. (2008) Structure and electrochemical properties of carbon aerogels synthesized at ambient temperatures as supercapacitors. Journal of Non-Crystalline So-

lids, 354, 19-24.

- [15] Prabakaran, S.R.S., Vimala, R., and Zainal, Z. (2006) Nanostructured mesoporous carbon as electrodes for supercapacitors. Journal of Power Sources, 161, 730-736.
- [16] Li, W., Pröbstle, H., and Fricke, J. (2003) Electrochemical behavior of mixed CmRF based carbon aerogels as electrode materials for supercapacitors. Journal of Non-Crystalline Solids, 325, 1-5.
- [17] Li, J., Wang, X., Huang, Q., Gamboa, S., and Sebastian, P.J. (2006) Studied on preparation and performances of carbon aerogel electrodes for the application of supercapacitor. Journal of Power Sources, 158, 784-788.
- [18] Xia, K., Gao, Q., Jiang, J., and Hu, J. (2008) Hierarchical porous carbons with controlled micropores and mesopores for supercapacitor electrode materials. Carbon, 46, 1718-1726.
- [19] Gamby, J., Taberna, P.L., Simon, P., Fauvarque, J.F., and Chesneau, M. (2001) Studies and characteristics of various activated carbons used for carbon/carbon supercapacitors. Journal of Power Sources, 101, 109-116.
- [20] Liu, X., Zhang, R., Zhan, L., Long, D., Qiao, W., Yang, J., and Ling, L. (2007) Impedance of carbon aerogel/activated carbon composites as electrodes of electrochemical capacitors in aprotic electrolyte. New Carbon Materials, 22, 153-158.
- [21] Dandekar, M.S., Arabale, G., and Vijayamohanan, K. (2005) Preparation and characterization of composite electrodes of coconut-shell-based activated carbon and hydrous ruthenium oxide for supercapacitors. Journal of Power Sources, 141, 198-203.
- [22] Hsieh, C. and Teng, H. (2002) Influence of oxygen treatment on electric double-layer capacitance of activated carbon fabrics. Carbon, 40, 667-674.
- [23] Honda, Y., Haramoto, T., Takeshige, M., Chiozaki, H., Kitamura, T., and Ishikawa, M. (2007) Aligned MWCNT sheet electrodes prepared by transfer methodology providing high-power capacitor performance. Electrochemical and Solid State Letters, 10, A106-A110.
- [24] He, X., Lei, J., Geng, Y., Zhang, X., Wu, M., and Zheng, M. (2009) Preparation of microporous activated carbon and its electrochemical

performance for electric double layer capacitor. Journal of Physics and Chemistry of Solids, 70, 738-744.

- [25] R. de Levie. (1963) On Porous Electrodes in Electrolyte Solutions. Electrochimica Acta, 8, 751-780.